

# The Application of a Dual Accelerometer Vector Sensor for the Discrimination of Seismic Reflections

A. Mantouka, P. Felisberto, S.M. Jesus, P. Santos  
LARSyS-SiPLAB, University of Algarve  
8005-139 Faro, Portugal  
Email:amantouka@ualg.pt

L. Sebastião, A. Pascoal  
LARSyS-ISR/IST, University of Lisbon  
1049-001 Lisbon, Portugal.

**Abstract**—This paper describes the application of a Dual Accelerometer Vector Sensor (DAVS) for the discrimination between the bottom reflections, the source direct arrival and the source ghost or multipath in an unconventional seismic acquisition scenario. The realisation of the DAVS device and the seismic acquisition scenario described in this paper, were carried out in the scope of the WiMUST project, an EU project, supported under the Horizon 2020 Framework Programme. The WiMUST project aims to improve the efficiency of the methodologies used to perform geophysical acoustic surveys at sea, using Autonomous Underwater Vehicles (AUVs) equipped with optimum sensors. In a classical reflection seismic survey scenario, the DAVS can contribute to this aim by steering its acoustic beam to the desired direction, therefore reducing the amount of post processing related to deghosting and multipath removal. Moreover, in an unconventional scenario, this steering capability offers the possibility of distinguishing between direct arrivals and multipath. In this paper, using data acquired during a WiMUST experiment, the device's directional estimation capabilities are demonstrated using a conventional beamformer for the determination of the Direction of Arrival (DOA) of seismic waves. The beamformer inputs are pressure and particle velocities in three directions. For the results presented here the pressure was derived from the devices' two accelerometers.

## I. INTRODUCTION

Acoustic vector sensors are relatively compact sensors with spatial filtering capabilities. In general, they are configured to measure acoustic pressure and particle velocity and combine these quantities to achieve an inherently directional beam. An important area of application for vector sensors is geo-acoustic surveys, where traditionally they are deployed on the earth surface or laid with cables on the seafloor. Owing to their directionality, they can distinguish between vertical and horizontal earth motions and hence they are used to record multicomponent seismic data. In marine surveys in particular, bottom cables with such sensors have been used for the attenuation of water-column reverberations [1]. In recent years, vector sensors have been used on ship-towed streamers for the elimination of surface reflections (ghosts) [2]; a further advancement in the area of marine seismic surveys is the installation of vector sensors on Autonomous Underwater Vehicles (AUVs), which tow streamers and perform remotely operated seismic surveys.

The EU project WiMUST (Widely scalable Mobile Underwater Sonar Technology) [3], supported under the Horizon

2020 Framework Programme, aims at expanding the functionalities of the current cooperative marine robotic systems, in order to enable deployment of distributed acoustic arrays for geophysical surveying in a scenario of a ship towing a source and receiving arrays (streamers) towed by AUVs. These arrays typically consist of pressure sensors, however adding and/ or replacing the hydrophone sensors with vector sensors is expected to be advantageous. Seismic processing for a variable geometry is challenging because the demands on positioning and synchronisation between many devices are high. To keep these unknowns under some control the first trial of the WiMUST project was carried out in a confined area of the Sines port, using two moored sparkers. Within this scenario, the Dual Accelerometer Vector Sensor (DAVS) was attached on a Medusa class AUV. Results from this trial in conjunction with vector sensor processing are discussed in section III-B.

## II. DAVS AND DOA ESTIMATION MODEL

The DAVS is an autonomously powered device, which consists of two tri-axial accelerometers and one hydrophone moulded in one unit. The device, as described in [4], has two main parts: (a) the acoustically active part (nose), which contains two tri-axial accelerometers and one hydrophone and (b) a container tube, which houses the electronics, the acquisition system and the batteries. Its total length of the device is 525 mm and its diameter is 65 mm. An exploded view of the three dimensional model of the device is shown in Fig.1. In this figure we discern, in the acoustically active part (in dark yellow, which represents the PolyUrethane (PU) mould), the DAVS sensing elements, which are two accelerometers (grey blocks) either side of the hydrophone (yellow cylindrical component). The accelerometers are moulded in the device so that both accelerometers face the same direction with the same sensitive face. For example, in the coordinate system shown here, both accelerometers have their sensitive X-face along the axis of the cylinder pointing to the nose of the device. These local coordinates are related to the 3-D space as follows: The X direction is in the direction of sail, the Y direction is the vertical direction pointing upwards and the Z-direction follows from the right-hand convention of the coordinate system.

In general, to beamform and beamsteer on this device, one accelerometer and the hydrophone are needed. However during

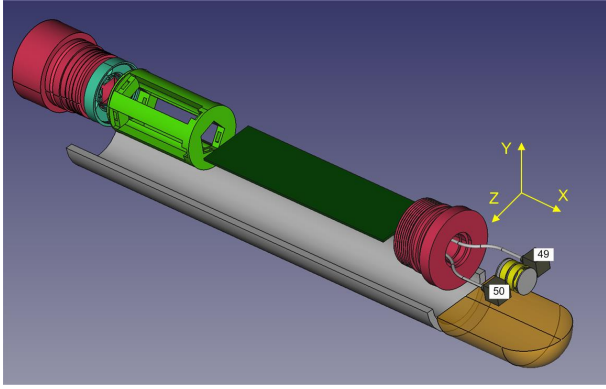


Fig. 1. Exploded view of DAVS, showing the container (white half tube), the acoustically active part (dark yellow), the two accelerometers (gray blocks), the hydrophone (yellow cylindrical component), the threaded caps (pink), the electronics (dark green block) and the battery pack (light green). The coordinate system indicates the Cartesian (local) coordinates of the device.

the trial described here, hydrophone data were not available and the pressure was computed from the two accelerometers. For the signal processing, the seismic arrival were considered plane waves travelling in a quiescent, homogeneous and isotropic fluid. Thus the relation between the acoustic pressure  $p$  and the particle velocity  $\vec{v}$  is

$$\vec{v} = \frac{p}{\rho c} \vec{u} \quad (1)$$

where the unit vector  $\vec{u}$  is pointing to the source and is expressed in terms of the azimuth ( $\theta$ ) and elevation ( $\phi$ ) angles

$$\vec{u} = \begin{bmatrix} \cos\theta\cos\phi \\ \sin\theta\cos\phi \\ \sin\phi \end{bmatrix} \quad (2)$$

Equation (1) allows the expression of velocity measurements in terms of equivalent acoustic pressure and source direction unit vector, by using the plane wave impedance ( $\rho c$ ) as the conversion factor (denoted here by  $z$ ).

For the single element beamforming, which was applied in this work, the pressure and the particle velocity time series were combined additively, following an approach similar to that described in [5]. That is, for a certain look direction  $\vec{u}$ , the output of the beamformer is

$$b(\vec{x}, t) = p(\vec{x}, t) + z\vec{v}(\vec{x}, t) \cdot \vec{u} \quad (3)$$

where the acoustic field variables are functions of both position in three-dimensional position  $\vec{x}$  and time  $t$ .

The acoustic pressure can be measured directly or as a derived value from the particle velocity differential. Combining the equation of state with the linearised equation of continuity, the acoustic pressure is related to the particle velocity gradient with

$$\frac{\partial p}{\partial t} + \rho c^2 (\nabla \cdot \vec{v}) = 0 \quad (4)$$

For the results shown in section III-B, the acoustic pressure was computed by converting (4) in frequency domain and

applying finite difference approximation to the velocity gradients. In that is, equation (4) was applied with the following approximation:

$$p \approx \frac{j\rho c^2}{\omega} \left[ \frac{\Delta v_x}{\Delta x} + \frac{\Delta v_y}{\Delta y} + \frac{\Delta v_z}{\Delta z} \right] \quad (5)$$

where  $v_x$ ,  $v_y$  and  $v_z$  are the three components of the acoustic particle velocity defined with (1) and  $\Delta v_x$  is the difference of the x-component of acoustic particle velocity derived by the two accelerometers which are separated by a distance  $\Delta x$ , similar definitions apply in the y and z directions.

### III. EXPERIMENT AND RESULTS

#### A. Sines trial

Seismic trials took place in the port of Sines, Portugal between 21-25 of November 2016. The area is protected from rough weather conditions and the sea bottom is basalt with a thin layer of mud on the top. During the experiment discussed here, two Medusa class AUVs were towing an eight-hydrophone streamer each; while two floating sparkers (with their tips been 30 cm below sea surface), either side of their tracks, were shooting alternatively every 0.5 s. The sparkers were operating at 200 J, giving a broadband pulse of about 1 ms with most of the energy concentrated in the frequency band 1 kHz - 2 kHz.

The DAVS was mounted on the yellow AUV shown in Fig. 2. During sailing it was positioned about 0.4 m below the surface. The geometry of the experiment is shown in figures 3 and 4; the first one shows the geometry and the distances discussed in this paper and the second one shows the same geometry superimposed with depth measurements. As it is discerned the bottom slopes from the shore towards the second sparker.

Both AUVs were sailing at surface with a nominal speed of 0.5 m/s, following the tracks shown in Fig. 4, where the orange markers indicate the position of the two sparkers. The first sparker (marked as SP1) was moored at a pontoon near the shore (not shown here), whilst the second sparker (marked as SP2) was in the middle of the port connected to an anchored ship at a depth of 23 m. The distances on the axis of Fig.3 and 4 are referenced with respect to the first sparker position.



Fig. 2. Photo of the AUV just after launching from a pontoon at Sines port; the DAVS is mounted on its lower part (showing in the photo as a white tube) which is submerged in the water. The orange cable is the connection between the streamer (not shown here) and the AUV.

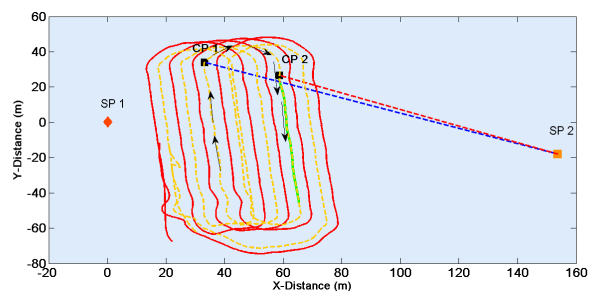


Fig. 3. Tracks sailed by the AUVs; in yellow the track sailed by the AUV carrying the DAVS. The orange markers show the position of the sparker. The black markers indicate the position of the yellow AUV for the first and second checkpoints respectively for the results discussed in section III-B; the arrows indicate the direction.

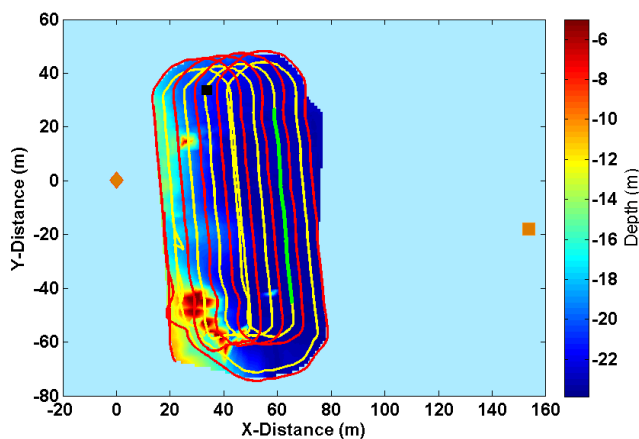


Fig. 4. Tracks sailed by the AUVs; in yellow the track sailed by the AUV carrying the DAVS. The orange markers indicate the sparker and the black one the AUV position for the first check point; the colorbar shows the depth below the area covered by the AUVs. The data acquired during sailing on the section of the track marked with green line were used to discuss seismic returns and produce Fig. 7.

### B. Discrimination of Seismic Arrivals

The results shown in this section are based on the application of the conventional (Bartlett) beamformer to the three signals from the accelerometer 49 and the derived pressure from accelerometers 49 and 50, see Fig. 1, using the theory of section II. The signals were band pass filtered between 1 kHz and 3.5 kHz. The azimuth angle of the beamformer is defined as the angle between the sensor and the sparker, on the horizontal plane parallel to the sea surface and the elevation angle is the grazing angle as seen by the sensor.

The data discussed here were acquired during the leg of the track marked with green line in Fig. 4 and 3 and the two check points (CP1 and CP2). With the AUV sailing in the direction indicated by the arrows, see Fig.3, it passed first through the first check point CP1, where the distance from the second sparker (blue line on Fig. 3) was about 131 m and the sea bottom slope between them is estimated to vary from 1m to 6 m (the depth values were obtained from

the AUV echo-sounder). With this geometry, it is expected to distinguish between the direct and the bottom reflected arrivals at the DAVS if there is enough time separation between the two arrivals. This is the case here because of the slope. Fig. 5 and Fig. 6 show the corresponding DOA estimates, normalised by the maximum of each occurrence from the first two distinguishable arrivals.

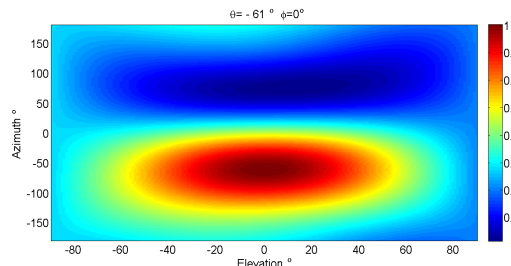


Fig. 5. DOA estimate of the direct arrivals at the first check point (CP1) of the AUV track.

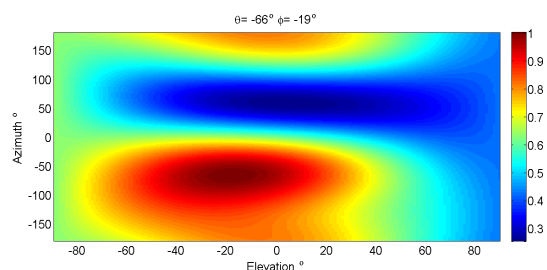


Fig. 6. DOA estimate of the bottom reflected arrival at the first check point (CP1) of the AUV track.

After this point, the AUV continued by turning on the race loop curve and entering a straight course marked in Fig. 4 and 3 with green line. At the beginning of this trajectory the DOA was computed for the second check point (CP2). Also for this part of the track, it was attempted to make a profile of the bottom using arrivals from the shots of the second sparker. For this part of the track the bottom is approximately flat, at a depth of 20 metres. The resulted intensity map of the returns is shown in Fig. 7, where on the horizontal axis is the distance travelled by the AUV and the vertical axis is the time elapsed from the time where the shot was fired. The intensity results are shown in dB scale after normalisation with the maximum occurrence.

For this track section, the direct and bottom reflected path have merged in one line, because, as the distance between source and sensor is approximately 104 m, (red line of Fig. 3), the time difference in terms of their arrival time is expected to be around 5 ms, which for the low frequency pulses used here it is difficult to be separated. For this reason the DOA estimate of the first arrival, shown in Fig. 8, is not representative of the true direction. The second line of Fig. 7 is a multipath with a time delay of approximately 0.02 s, which for this geometry is roughly the multiple over the distance of one depth. This is

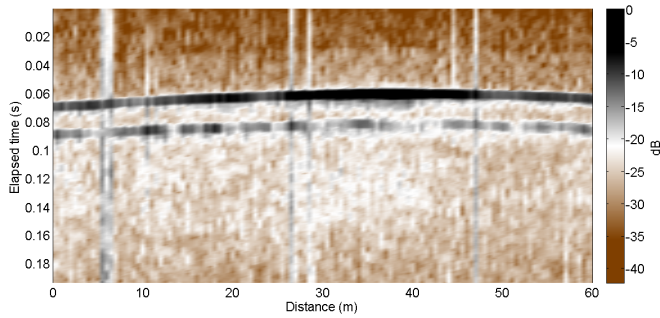


Fig. 7. Intensity map of arrival during sailing on the track leg marked with green line Fig.4; showing the direct arrival merged with the bottom reflected one and the first multipath source ghost.

supported by the DOA estimate, shown in Fig. 9, where the elevation is positive indicating that the reflection comes from the surface.

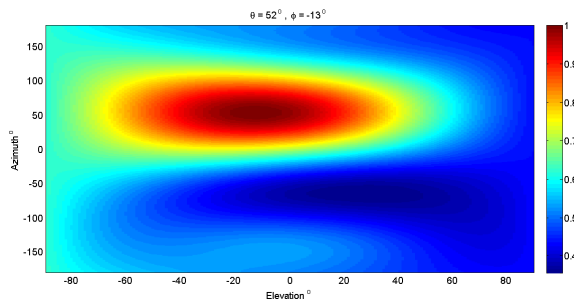


Fig. 8. DOA estimate of the first arrival at CP2, shown in Fig.3.

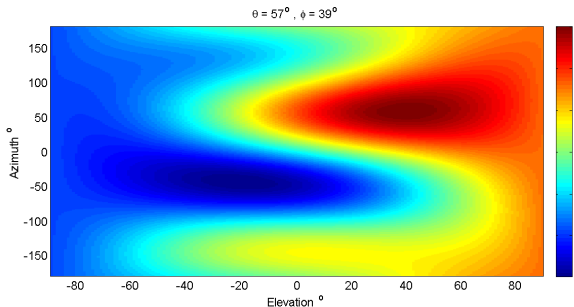


Fig. 9. DOA estimate of the second arrival at CP2, shown in Fig.3.

#### IV. CONCLUSION

This paper showed experimental results in connection with the potential of a single vector sensor to discriminate the bottom seismic reflections from the direct path and the multipath surface reflected arrivals; when the minimum time-space separation between pulses allows. Seismic returns, presented as an intensity map using a single sensor, suggested the advantage of these sensors over simple hydrophones. Such a picture would be difficult to be produced with a single

hydrophone. However, a tri-axial vector sensor, in spite of its relative wide beam, has the potential to steer the beam in the desired direction and produce results that otherwise could only be obtained with an array of hydrophones. Future work involves further development of the algorithm for seismic surveys with AUVs and the deployment of more than one vector sensor for bottom and sub-bottom profiling.

#### ACKNOWLEDGEMENT

This work is funded from the European Union Horizon 2020 research and innovation programme under grant agreement No. 645141 (WiMUST project)

#### REFERENCES

- [1] F. J. Barr, J. I. Sanders, *et al.*, "Attenuation of water-column reverberations using pressure and velocity detectors in a water-bottom cable," in *1989 SEG Annual Meeting*, Society of Exploration Geophysicists, 1989.
- [2] M. Widmaier, E. Fromyr, and V. Dirks, "Dual-sensor towed streamer: from concept to fleet-wide technology platform," *first break*, vol. 33, no. 11, pp. 83–89, 2015.
- [3] H. Al-Khatib, G. Antonelli, A. Caffaz, A. Caiti, G. Casalino, I. B. de Jong, H. Duarte, G. Indiveri, S. Jesus, K. Kebkal, *et al.*, "Navigation, guidance and control of underwater vehicles within the widely scalable mobile underwater sonar technology project: an overview," *IFAC-PapersOnLine*, vol. 48, no. 2, pp. 189–193, 2015.
- [4] A. Mantouka, P. Felisberto, P. Santos, D. Maslov, F. Zabel, M. Saleiro, S. M. Jesus, and L. Sebastião, "Development and testing of a dual accelerometer vector sensor for auv acoustic surveys," in *The 3rd International Electronic Conference on Sensors and Applications (ECSA 2016)*, 1530 November 2016; *Sciforum Electronic Conference Series*, vol. 1, 2016.
- [5] G. D'Spain, W. Hodgkiss, G. Edmonds, J. Nickles, F. Fisher, and R. Harriss, "Initial analysis of the data from the vertical difar array," in *OCEANS'92. Mastering the Oceans Through Technology. Proceedings.*, vol. 1, pp. 346–351, IEEE, 1992.